ISSN: 0975-8585

Research Journal of Pharmaceutical, Biological and Chemical Sciences

A Quantum Chemical Study of the Relationships between Electronic Structure and cloned rat 5-HT_{2C} Receptor Binding Affinity in N-Benzylphenethylamines.

Juan S. Gómez-Jeria*, and Andrés Robles-Navarro.

Quantum Pharmacology Unit, Department of Chemistry, Faculty of Sciences, University of Chile. Las Palmeras 3425, Santiago 7800003, Chile.

ABSTRACT

We analyzed the relationships between the electronic structure and cloned rat 5-HT_{2C} receptor binding affinity for a large group of N-Benzylphenethylamines. The electronic structure of the molecules was obtained at the B3LYP/6-31G(d,p) level with full geometry optimization. Three statistically significant equations were obtained. From them the requirements for a high affinity were inferred. The partial interaction pharmacophores, containing information for the synthesis of new molecular systems with enhanced affinity, are proposed.

Keywords: 5-HT_{2C} receptor, QSAR, DFT, serotonin, receptor binding affinity, docking, *N*-benzylphenethylamines, chemical reactivity, local reactivity indices.

Corresponding author

ISSN: 0975-8585

INTRODUCTION

The 5-HT_{2C} receptor is one of the various binding sites for serotonin. 5-HT_{2C} receptors are strongly expressed all through the CNS and are expressed at minor levels outside the brain [1]. 5-HT_{2C} receptors regulate dopamine release in, for example, the amygdala, hippocampus, hypothalamus, nucleus accumbens, prefrontal cortex and the striatum. 5-HT_{2C} receptors are claimed to significantly regulate mood, anxiety, obesity, cognition, appetite, addiction, antipsychotic drug actions and reproductive behavior [1-25]. Also a certain number of suicide victims have an unusually high number of 5-HT_{2C} receptors in their prefrontal cortex. Several groups of molecules binding to 5-HT_{2C} receptors have been synthesized and tested [20, 26-49]. Recently we carried out docking and structure-affinity studies for a group of N-Benzylphenethylamines interacting with 5-HT_{2A} and 5-HT_{2B} receptors. To complete the study of these molecules we present here the results of a quantum-chemical analysis of the relationships between the electronic structure and the cloned rat 5-HT_{2C} receptor binding affinity of the above mentioned molecules.

METHODS, MODELS AND CALCULATIONS

As this is the third part of a study we refer the reader to the previous papers and other references for more details about the formal method employed here [50-56]. In summary, the receptor binding affinity, pK, can be expressed by the following linear expression:

$$pK_i = a + \sum_j \left[e_j Q_j + f_j S_j^E + s_j S_j^N \right] +$$
$$+ \sum_j \sum_m \left[h_j(m) F_j(m) + x_j(m) S_j^E(m) \right] + + \sum_j \sum_{m'} \left[r_j(m') F_j(m') + t_j(m') S_j^N(m') \right] +$$
$$+ \sum_j \left[g_j \mu_j + k_j \eta_j + o_j \omega_j + z_j \varsigma_j + w_j Q_j^{\max} \right] + \sum_{B=1}^{W} O_B \qquad (1)$$

where Q_i is the net charge of atom j, S_j^E and S_j^N are the total atomic electrophilic and nucleophilic superdelocalizabilities of Fukui, $F_{j,m}$ ($F_{j,m'}$) is the Fukui index of the occupied (empty) MO m (m') localized on atom j. $S_j^E(m)$ is the atomic electrophilic superdelocalizability of MO m on atom j, etc. The total atomic electrophilic superdelocalizability of atom j is the sum over occupied MOs of the $S_j^E(m)$'s and the total atomic nucleophilic superdelocalizability of atom j is the sum over empty MOs of the $S_j^N(m)$'s. The last bracket of the right side of Eq. 1 contains a novel set of local atomic reactivity indices obtained from the Hartree-Fock LCAO-MO and DFT models. Hereafter, $HOMO_j$* refers to the highest occupied molecular orbital localized on atom j and $LUMO_j$* to the lowest empty MO localized on atom j. μ_j is the local atomic electronic chemical potential of atom j ($HOMO_j$*-$LUMO_j$* midpoint), η_j is the local atomic hardness of atom j ($HOMO_j$*-$LUMO_j$* gap), ω_j is the local atomic electrophilicity of atom j, ς_j is the local atomic softness of atom j and $Q_j^{\max}$ is the maximal amount of electronic charge that atom j may accept. The moment of inertia term of Eq. 1 can be expressed as:

$$\log\left[(ABC)^{-1/2} \right] = \sum_i \sum_t m_{i,t} R_{i,t}^2 = \sum_t O_t \qquad (2)$$

where the summation on t is over the different substituents of the molecule, $m_{i,t}$ is the mass of the i-th atom belonging to the t-th substituent, $R_{i,t}$ being its distance to the atom to which the substituent is attached. These terms represent the fraction of molecules attaining the right orientation to interact with the receptor. We called them orientation parameters. The application of this method to affinity constants [53, 57-74] and other kinds of biological activities [75-97] has given excellent results. The selected molecules are shown in Fig. 1 and Table 1 [98].

ISSN: 0975-8585

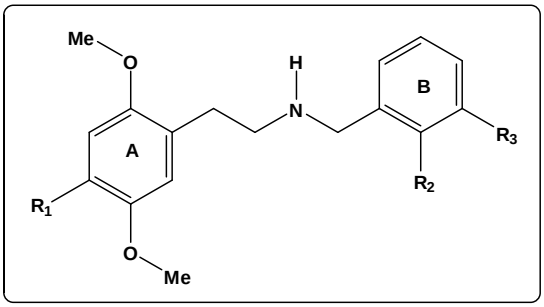

Figure 1. General formula of N-Benzylphenethylamines.

Table 1. Selected N-Benzylphenethylamines*.

Mol.	R_1	R_2	R_3	Mol.	R_1	R_2	R_3
1	Br	OMe	H	23	Pr	F	H
2	Br	OH	H	24	Pr	O-CH_2-O	
3	Br	F	H	25	SMe	OMe	H
4	Br	O-CH_2-O		26	SMe	OH	H
5	Cl	OMe	H	27	SMe	F	H
6	Cl	OH	H	28	SMe	O-CH_2-O	
7	Cl	F	H	29	SEt	OMe	H
8	Cl	O-CH_2-O		30	SEt	OH	H
9	F	OMe	H	31	SEt	F	H
10	F	OH	H	32	SEt	O-CH_2-O	
11	F	F	H	33	SPr	OMe	H
12	F	O-CH_2-O		34	SPr	OH	H
13	Me	OMe	H	35	SPr	F	H
14	Me	OH	H	36	SPr	O-CH_2-O	
15	Me	F	H	37	CF_3	OMe	H
16	Me	O-CH_2-O		38	CF_3	OH	H
17	Et	OMe	H	39	CF_3	F	H
18	Et	OH	H	40	CF_3	O-CH_2-O	
19	Et	F	H	41	CN	OMe	H
20	Et	O-CH_2-O		42	CN	OH	H
21	Pr	OMe	H	43	CN	F	H
22	Pr	OH	H	44	CN	O-CH_2-O	

* Molecule 41 was not employed due to convergence problems during the geometry optimization process.

As in the previous papers dealing with 5-HT_{2A} and 5-HT_{2B} receptors, we considered three different groups of molecules: the entire set (n=43, set I), a second set in which the R_1 substituent is an alkyl moiety (molecules 13-24 and 37-40, n=16, set II) and a third set in which R_1 is halogen, S-alkyl or CN (molecules 1-12, 25-36 and 42-44, n=27, set III). The common skeleton for all sets is shown in Fig. 2.

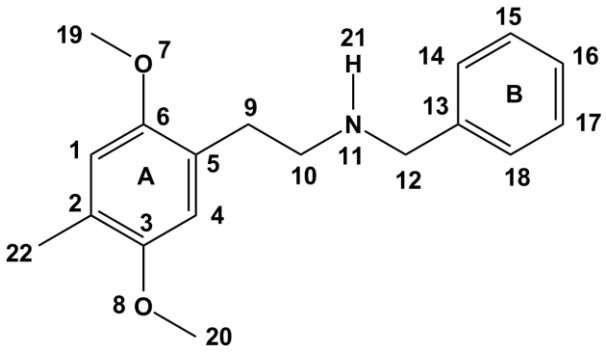

Figure 2. Numbering of the common skeleton.

In addition to rings A and B and the heavy atoms of the linker joining them, we included as part of the common skeleton one of the N protons, the oxygen and carbon atoms of both OMe substituents and the first

atom attached to position 22 in Fig. 2. The biological activity selected is the ability of these compounds to displace [3H]-mesulergine at 5-HT_{2C} cloned rat receptors [98]. These data are expressed as pK and it is shown in Table 2.

Table 2. N-Benzylphenethylamines derivatives and binding affinities.

Mol.	pK 5-HT_{2C}	Mol.	pK 5-HT_{2C}
1	8.77	23	7.88
2	8.33	24	8.13
3	7.73	25	8.15
4	7.95	26	8.29
5	8.27	27	7.16
6	8.21	28	7.56
7	7.43	29	8.65
8	7.67	30	8.72
9	7.36	31	7.64
10	7.16	32	8.04
11	6.31	33	8.71
12	6.59	34	8.66
13	8.23	35	7.84
14	7.92	36	8.06
15	7.18	37	8.57
16	7.43	38	8.49
17	8.55	39	7.74
18	8.47	40	7.93
19	7.58	41	7.25
20	7.92	42	6.88
21	8.79	43	6.2
22	8.51	44	6.86

CALCULATIONS

All calculations were done for the protonated form. The calculation procedure was done as in the two related papers [73, 74]: geometries were fully optimized within the B3LYP/6-31G(d,p) framework with the Gaussian suite of programs [99]. From the single point result we corrected the Mulliken Population Analysis and calculated all the necessary local atomic reactivity indices with the D-CENT-QSAR program [100, 101]. Molecular electrostatic potentials and molecular orbitals (MO) were depicted with GaussView and Molekel, and conformers were calculated with MarvinView [102-104]. As there are no enough cases to solve the system of equations 1, we carried out a linear multiple regression analysis (LMRA) with the Statistica software [105].

RESULTS

Results for the whole set of molecules (I)

Results for the 5-HT_{2C} binding affinity of the whole set of molecules (I)

No statistically significant equation was obtained for the whole set. Extracting one by one the cases producing outliers we finally obtained:

$$pK_i = -31.83 - 1.30S_3^E - 3.62S_{13}^E - 3.47S_{20}^E(HOMO)* + \\ +17.28\eta_2 + 0.78F_{15}(HOMO-1)* - 3.63\mu_{22} + 0.90F_{17}(LUMO)* \quad (2)$$

with n=36, R= 0.99, R^2= 0.98, adj-R^2= 0.98, F(7,28)=208.75 (p<0.00001) and a standard error of estimate of 0.11. No outliers were detected and no residuals fall outside the ±2.00 σ limits. Here, S_3^E is the total atomic electrophilic superdelocalizability of atom 3 (in ring A), S_{13}^E is the total atomic electrophilic superdelocalizability of atom 13 (in ring B), $S_{20}^E(HOMO)*$ is the orbital electrophilic superdelocalizability of the highest occupied MO localized on atom 20 (a carbon atom of a MeO substituent), η_2 is the local atomic hardness of atom 2 (in ring A), $F_{15}(HOMO-1)*$ is the Fukui index of the second highest occupied MO localized on atom 15 (in ring B), μ_{22} is the local atomic electronic chemical potential of atom 22 (the atom directly bonded to position 2) and $F_{17}(LUMO)*$ is the Fukui index of the lowest vacant MO localized on atom 17 (in ring B). Tables 3 and 4 show, respectively, the beta coefficients, the results of the t-test for significance of coefficients and the matrix of squared correlation coefficients for the variables appearing in Eq. 2. Figure 3 shows the plot of observed *vs.* calculated values.

Table 3. Beta coefficients and t-test for significance of coefficients in Eq. 2.

	Beta	t(28)	p-level
S_3^E	-0.82	-26.04	<0.000001
S_{13}^E	-0.47	-14.29	<0.000001
$S_{20}^E(HOMO)*$	-0.25	-8.01	<0.000001
η_2	0.22	6.84	<0.000001
$F_{15}(HOMO-1)*$	0.16	5.80	<0.000003
μ_{22}	-0.14	-5.30	<0.00001
$F_{17}(LUMO)*$	0.08	**2.45**	**<0.02**

Table 4. Matrix of squared correlation coefficients for the variables in Eq. 2.

	S_3^E	S_{13}^E	$S_{20}^E(HOMO)*$	η_2	$F_{15}(HOMO-1)*$	μ_{22}
S_{13}^E	0.05	1.00				
$S_{20}^E(HOMO)*$	0.22	0.004	1.00			
η_2	0.12	0.06	0.16	1.00		
$F_{15}(HOMO-1)*$	0.002	0.005	0.005	0.01	1.00	
μ_{22}	0.03	0.04	0.03	0.003	0.001	1.00
$F_{17}(LUMO)*$	0.008	0.19	0.005	0.0009	0.04	0.01

ISSN: 0975-8585

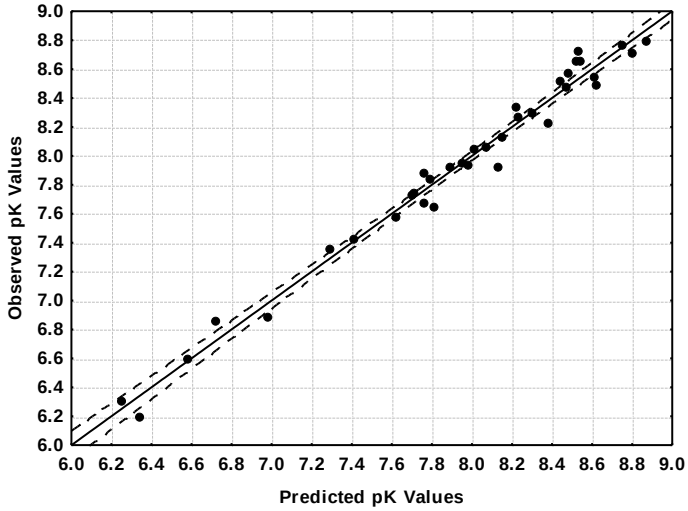

Figure 3. Plot of predicted *vs*. observed pK values (Eq. 2). Dashed lines denote the 95% confidence interval.

Table 9 shows that there are no significant internal correlations between independent variables. The associated statistical parameters of Eq. 2 show that this equation is statistically significant and that the variation of a group of seven local atomic reactivity indices belonging to the common skeleton explains about 98% of the variation of the 5-HT_{2C} receptor binding affinity. Figure 3, spanning almost 2.6 orders of magnitude, shows that there is a good correlation of observed *versus* calculated values and that almost all points are inside the 95% confidence interval.

Results for the set II of molecules

Results for 5-HT_{2C} binding affinity of set II.

The whole set LMRA analysis detected one outlier. After extracting the corresponding case, the following statistically significant equation was obtained:

$$pK_i = -24.16 - 4.55S_{13}^{E} + 0.002\phi_{R1} \quad (3)$$

with n=15, R= 0.97, R^2= 0.95, adjusted R^2= 0.94, F(2,12)=114.52 (p<0.00000) and a standard error of estimate of 0.11. No outliers were detected and no residuals fall outside the ±2.00 σ limits. Here, ϕ_{R1} is the orientational parameter of the R_1 substituent and S_{13}^{E} is the total atomic electrophilic superdelocalizability of atom 13 (in ring B). Tables 5 and 6 show, respectively, the beta coefficients, the results of the t-test for significance of coefficients and the matrix of squared correlation coefficients for the variables appearing in Eq. 3. Figure 4 shows the plot of observed *vs.* calculated values.

Table 5. Beta coefficients and t-test for significance of coefficients in Eq. 3.

	Beta	t(12)	p-level
S_{13}^{E}	-0.89	-13.66	<0.000001
ϕ_{R1}	0.56	8.62	<0.000002

Table 6. Matrix of squared correlation coefficients for the variables in Eq. 3.

	S_{13}^{E}
ϕ_{R1}	0.03

ISSN: 0975-8585

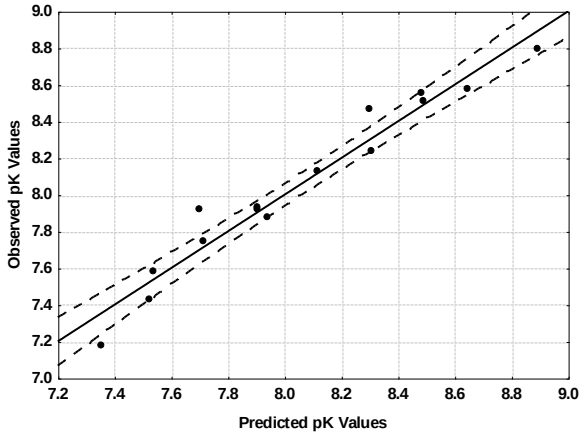

Figure 4. Plot of predicted *vs*. observed pK values (Eq. 3). Dashed lines denote the 95% confidence interval.

Table 15 shows that there are no significant internal correlations between independent variables. The associated statistical parameters of Eq. 3 show that this equation is statistically significant and that the variation of a group of two local atomic reactivity indices belonging to the common skeleton explains about 94% of the variation of the 5-HT_{2C} receptor binding affinity. Figure 4, spanning about 1.6 orders of magnitude, shows that there is a good correlation of observed *versus* calculated values and that almost all points are inside the 95% confidence interval.

Results for the set III of molecules

Results for 5-HT_{2C} binding affinity of set II.

Two outliers were detected in the first two LMRA results. Once the corresponding cases were eliminated the following statistically significant equation was obtained:

$$pK_i = -29.31 - 0.67S_{22}^{E}(HOMO-1)^{*} - 5.66S_{12}^{E} + 6.29S_{10}^{E}(HOMO-1)^{*} \quad (4)$$

with n=25, R= 0.97, R^2= 0.94, adjusted R^2= 0.94, F(3,21)=117.66 (p<0.000001) and a standard error of estimate of 0.19. No outliers were detected and no residuals fall outside the ±2.00 σ limits. Here, $S_{22}^{E}(HOMO-1)^{*}$ is the orbital electrophilic superdelocalizability of the second highest occupied MO localized on atom 22 (the atom directly bonded to position 2 in ring A), S_{12}^{E} is the total electrophilic superdelocalizability of atom 12 (the carbon atom of the NH-ring B linker) and $S_{10}^{E}(HOMO-1)^{*}$ is the orbital electrophilic superdelocalizability of the second highest occupied MO localized on atom 10 (one of the carbon atoms of the NH-ring A linker).
Tables 7 and 8 show, respectively, the beta coefficients, the results of the t-test for significance of coefficients and the matrix of squared correlation coefficients for the variables appearing in Eq. 4. Figure 5 shows the plot of observed *vs.* calculated values.

Table 7. Beta coefficients and t-test for significance of coefficients in Eq. 4.

	Beta	t(21)	p-level
$S_{22}^{E}(HOMO-1)^{*}$	-0.68	-12.68	<0.000001
S_{12}^{E}	-0.53	-9.96	<0.000001
$S_{10}^{E}(HOMO-1)^{*}$	0.19	3.73	<0.001

ISSN: 0975-8585

Table 8. Matrix of squared correlation coefficients for the variables in Eq. 4.

	$S_{22}^{E}(HOMO-1)*$	S_{12}^{E}
S_{12}^{E}	0.004	1.00
$S_{10}^{E}(HOMO-1)*$	0.0004	0.009

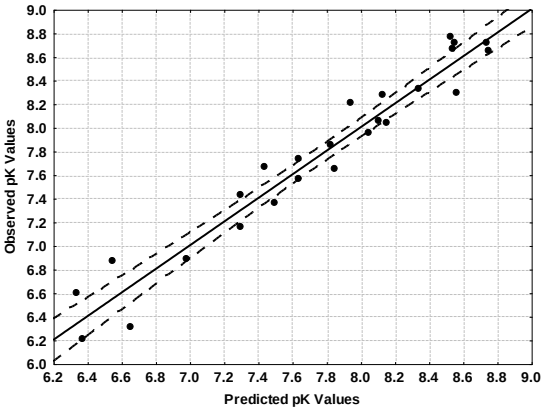

Figure 5. Plot of predicted *vs*. observed pK values (Eq. 4). Dashed lines denote the 95% confidence interval.

Table 8 shows that there are no significant internal correlations between independent variables. The associated statistical parameters of Eq. 4 show that this equation is statistically significant and that the variation of a group of three local atomic reactivity indices belonging to the common skeleton explains about 94% of the variation of the 5-HT_{2C} receptor binding affinity. Figure 5, spanning about 2.5 orders of magnitude, shows that there is a good correlation of observed *versus* calculated values and that almost all points are inside the 95% confidence interval.

DISCUSSION

It is the *simultaneous* variation of all the numerical values of the LARIs appearing in the equations which explains the variation of the activity through the group. Those reactivity indices of atoms participating in the interaction but having a constant numerical value in all molecules will not appear in the LRMA equations. This is the major reason to employ the term "*partial pharmacophore*" to represent the pharmacophores built from these kinds of results. Also, all molecular orbital-related LARIs employed here (Fukui indices and orbital superdelocalizabilities) have non-zero values (this is so because of the way we build the data matrix, see [68]). Therefore, it is of common sense to accept that if an occupied MO different from the HOMO and localized on a particular atom appears in the equations, the occupied MOs having a lower energy and localized on the same atom also participate in the interaction. An analysis is carried out employing the *variable-by-variable* (VbV) method: the conditions that a particular reactivity index must fulfill for a high pK_i are determined and the corresponding interaction or interactions are proposed. In the case of the orbital-related LARIs the nature (σ, π, lone pair, etc.) of the MOs must be taken into account. In the case of the local MO structures of atoms appearing in Eq. 2-4 (atoms 10, 15, 17, 20 and 22), they have been tabulated in Refs. [73, 74].

Discussion of the results for the 5-HT_{2C} binding affinity of the whole set of molecules

The beta values (Table 3) show that the relative importance of these indices is S_3^E >> S_{13}^E > > $S_{20}^E(HOMO)*$ > η_2 > $F_{15}(HOMO-1)*$ > μ_{22} > $F_{17}(LUMO)*$. A VbV analysis of Eq. 2 shows that a high pK value is associated with high values for S_3^E, S_{13}^E, $S_{20}^E(HOMO)*$, η_2, $F_{15}(HOMO\text{-}1)*$ and $F_{17}(LUMO)*$, and with a highly negative value for μ_{22}. Atoms 3 and 13 are carbon atoms belonging, respectively, to rings A and B (Fig. 2). High values for S_3^E and S_{13}^E suggest that these atoms are interacting with electron-acceptor centers (π-cation, π-alkyl and/or carbon H-bond interactions). In general a carbon H-bond

has the form C-H….O). Atom 2 is a carbon in ring A. A high value for η_2 (the $(HOMO)^*_2$-$(LUMO)^*_2$ energy gap) is needed for a high binding affinity. The enlargement of this gap allows suggesting that this atom is not interacting with charged groups. Possible interactions are π-π, π-alkyl and/or π-σ. Atom 20 is the carbon atom of the OMe substituent attached to atom 3 of ring A (see Fig. 2). All MOs of this atom are of σ nature ([73], Table 3). Then a high value for $S^E_{20}(HOMO)^*$ is an indication that the σ electrons are interacting with an appropriate partner through σ-π, σ-σ and/or carbon H bonds. Atoms 15 and 17 are carbon atoms belonging to ring B (see Fig. 2). In the case of atom 15 $(HOMO\text{-}1)^*_{15}$ can be of σ or π nature. $(HOMO)^*_{15}$ is a π MO in all cases. In the case of a π $(HOMO\text{-}1)^*_{15}$ it is possible to suggest that atom 15 is involved in π-π, π-amide and/or π-σ interactions employing its first two occupied MOs. For the case of a σ $(HOMO\text{-}1)^*_{15}$ we suggest a secondary interaction with an appropriate site (σ-π and/or σ-σ interactions). $(LUMO)^*_{17}$ is a π MO in all cases. A high value for $F_{17}(LUMO)^*$ could be an indication that this atom is interacting with an electron-rich center (allowing π-π stacking and/or π-anion interactions). Atom 22 is directly attached to position 2 of ring A (see Fig. 2). Its nature is very different as shown in Table 1. μ_{22} is the midpoint of the $(HOMO)^*_{22}$-$(LUMO)^*_{22}$ energy gap. Accepting that the correct form to obtain a more negative value for μ_{22} is by lowering the $(LUMO)^*_{22}$ energy, a preliminary interpretation of the requirements for this reactivity index is that atom 22 interacts with an electron-rich center like atom 17. All these ideas are summarized in the two-dimensional (2D) partial interaction pharmacophore depicted in Fig. 6.

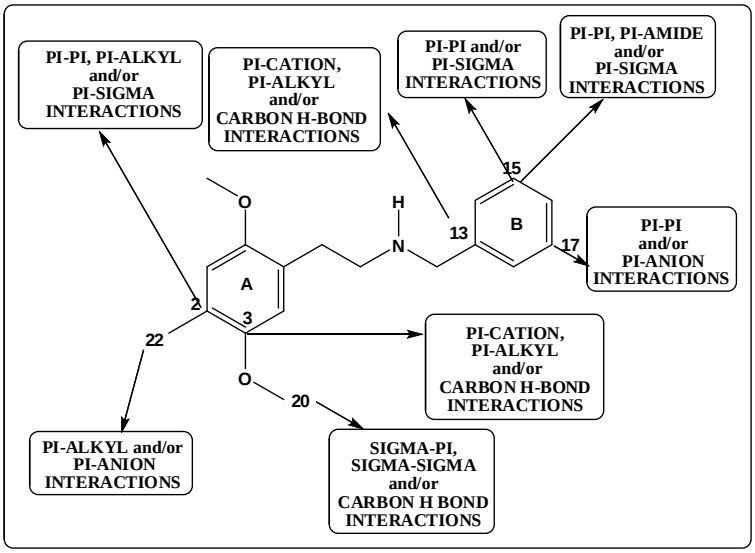

Figure 6. 2D partial interaction pharmacophore for Ec. 3.

Discussion of the results for 5-HT$_{2C}$ binding affinity of set II

The beta values (Table 5) show that the relative importance of these indices is S^E_{13} >> ϕ_{R1} . The VbV analysis of Eq. 3 shows that a high receptor affinity is associated with high values for S^E_{13} and ϕ_{R1} . Atom 13 is a carbon atom in ring B (see Fig. 2). As in the previous case, the required high value for S^E_{13} indicates that this atom is interacting with an electron-deficient center (proposed interactions: π-cation, π-alkyl and/or carbon H-bond). ϕ_{R1} is a purely geometrical reactivity index [53, 54]. In this set the R_1 substituent is an alkyl moiety (fluorinated in some cases). Interestingly, in our previous QSAR studies with this same set of molecules interacting with 5-HT$_{2A}$ and 5-HT$_{2B}$ receptors no orientational parameters appeared in the equations for this set [73, 74]. As a high value for ϕ_{R1} is required, it is possible to suggest that a longer and/or branched alkyl substituent can enhance the receptor binding affinity. This will not affect the electronic structure of ring A, but

we must not forget that it is possible that for longer alkyl substituents σ-σ interactions may appear. These conditions are shown in the 2D partial interaction pharmacophore of Fig. 7.

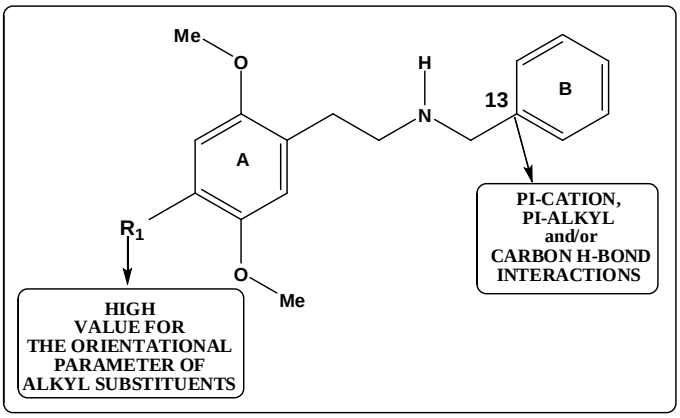

Figure 7. 2D partial interaction pharmacophore for Ec. 3.

Discussion of the results for 5-HT$_{2C}$ binding affinity of set III

The beta values (Table 7) show that the relative importance of these indices is $S_{22}^{E}(HOMO-1)^{*}$ > S_{12}^{E} >> $S_{10}^{E}(HOMO-1)^{*}$. A VbV analysis of Eq. 4 shows that a high pK value is associated with high values for $S_{22}^{E}(\text{HOMO-1})^{*}$ and S_{12}^{E}, and a small value for $S_{10}^{E}(\text{HOMO-1})^{*}$. Atom 12 is a carbon linking the N atom with the B ring (see Fig. 2). All MOs are of σ nature. A high value for S_{12}^{E} indicates that σ electrons of atom 12 are involved in interactions with other electrons (σ-π and/or σ-σ interactions and/or carbon H bonds) and/or with π systems (σ-π interactions). Atom 22 is the atom attached to position 2 of ring A (see Fig. 2). $(\text{HOMO-1})_{22}^{*}$ and $(\text{HOMO})_{22}^{*}$ can be of π, σ or lone pair nature (see Table 10 in Ref. [74]). A high value for $S_{22}^{E}(\text{HOMO-1})^{*}$ could be an indication of a favorable interaction with an electron-deficient center. Atom 10 is a carbon atom bonded to the N atom and belonging to the chain linking this atom to ring A. The MOs of this atom are all of σ nature. A small value for $S_{10}^{E}(\text{HOMO-1})^{*}$ suggests the possibility of a repulsive (unfavorable) interaction between these σ electrons and other electrons present in the receptor such as σ electrons of alkyl groups and/or π electrons. These suggestions are represented in the 2D partial interaction pharmacophore of Fig. 8.

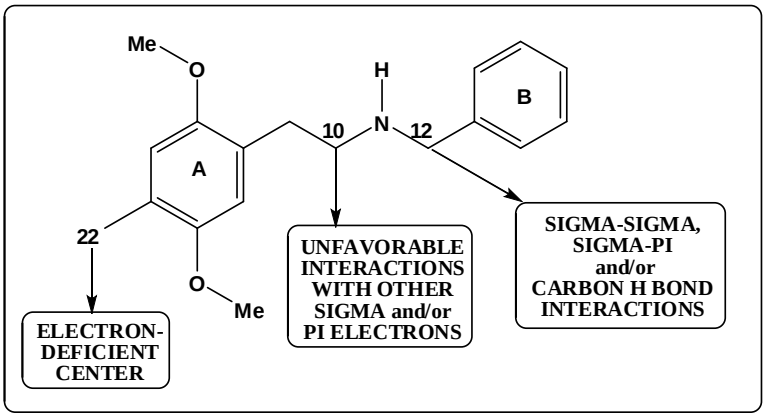

Figure 8. 2D partial interaction pharmacophore for Ec. 4.

The comparison of these three partial interaction pharmacophores shows that they do not have contradictory information. A final partial pharmacophore, shown in Fig. 9, was obtained by merging Figs. 6-8.

ISSN: 0975-8585

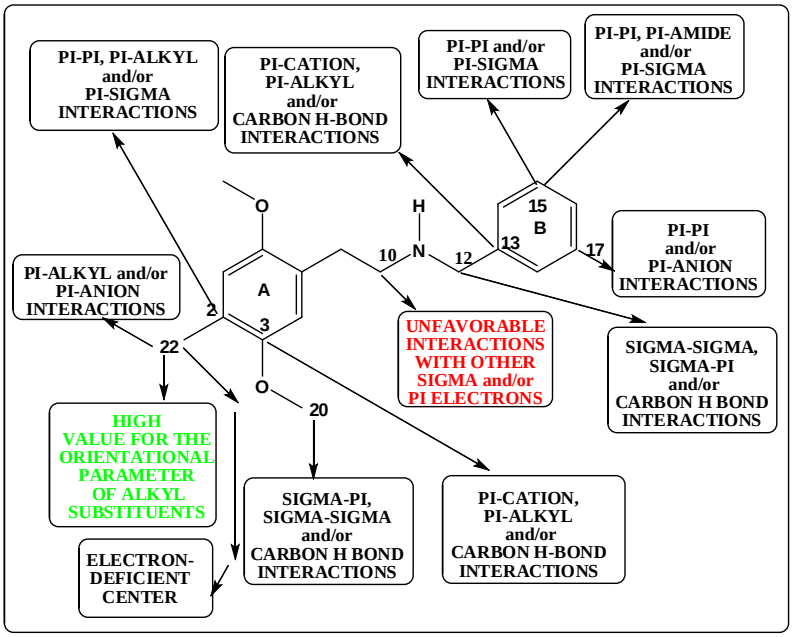

Figure 9. Final partial 2D interaction pharmacophore.

It is interesting to notice that in the QSAR results for the same molecules interacting with 5-HT_{2A} and 5-HT_{2B} receptors no orientational parameter of the substituent attached to atom 2 (see Fig. 9) appeared in the resulting equations. One of the possible explanations is that the binding site of the 5-HT_{2C} receptor could be more exposed to the external milieu than the binding sited of 5-HT_{2A} and 5-HT_{2B} receptors.

MOLECULAR ELECTROSTATIC POTENTIAL

These molecules act in a protonated form. Fig. 10 shows, as an example, the MEP structure of molecules 9-12 in their fully optimized geometry (calculations of similar systems are presented in Refs. [57, 106]).

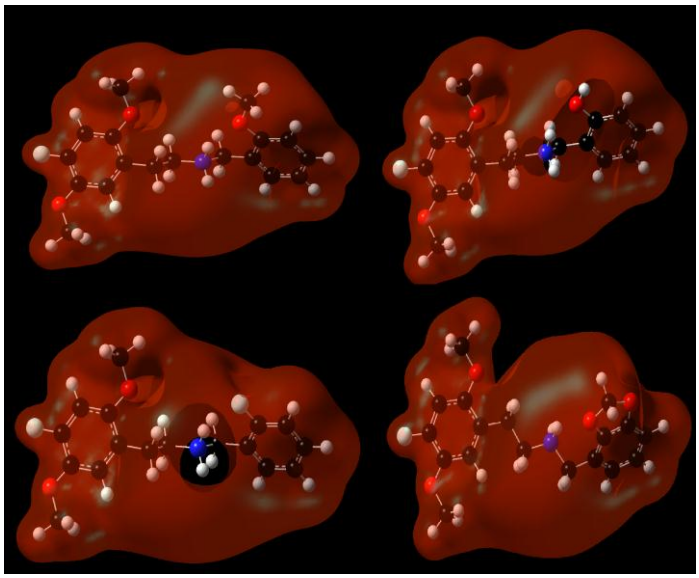

Figure 10. MEP map of molecules 9 (upper left), 10 (upper right), 11 (lower left) and 12 (lower right). The red isovalue surface corresponds to positive MEP values (0.1).

We can see that protonation produces MEP maps without negative areas as expected. Fig. 11 displays the MEP map of molecules 9-12 at 4.5 Å of the nuclei.

ISSN: 0975-8585

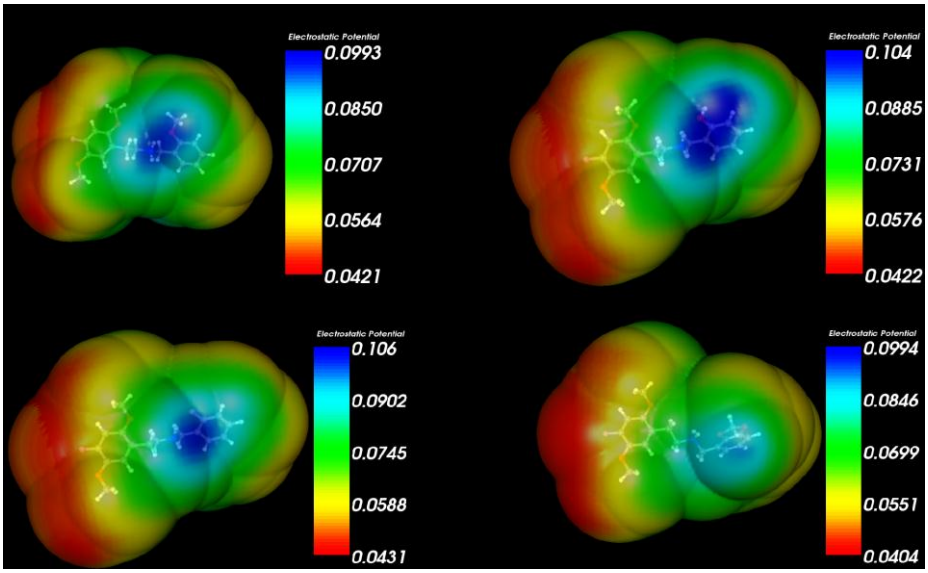

Figure 11. MEP map of molecules 9 (upper left), 10 (upper right), 1 (lower left) and 12 (lower right) at 4.5 Å of the nuclei.

We can see that at 4.5 Å the MEP values are positive and that the zones having the highest positive values are located between the proton and ring B. As we do not know the receptor's structure it is not possible to suggest the form in which the molecule approaches its binding site.

MOLECULAR ORBITALS

We shall provide here examples helping to understand the concept of Local Molecular Orbitals. The central problem is to determinate when a given MO can be considered as localized on a certain atom. Using pictorial depictions of the MOs is a bad procedure because it depends on the isovalues chosen to represent them. As an extreme example, we present in Fig 12 the HOMO of molecule 4 displayed at different isovalues.

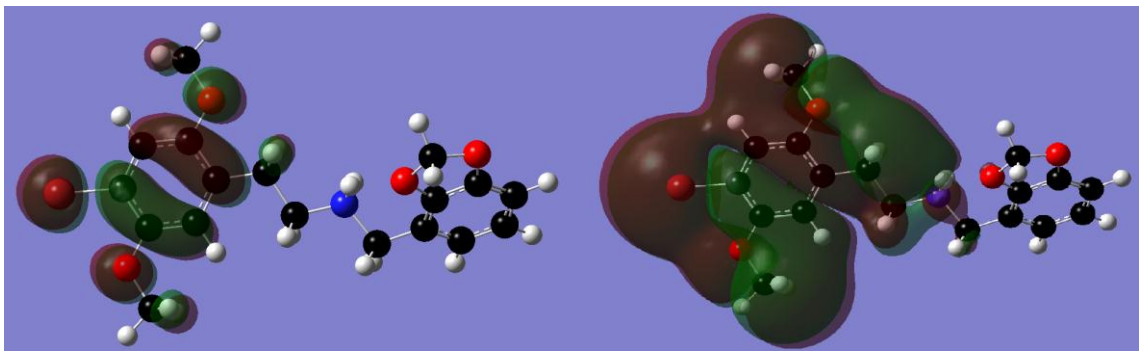

Figure 12. HOMO of molecule 4 at isovalues of 0.02 e/au^3 (left) and 0.001 e/au^3 (right).

We can observe that for smaller isovalues we get more extended density maps. Then, it seems necessary to employ a kind of quantitative measurement allowing us to provide an answer for the aforementioned question. For reasons exposed earlier [56] we consider that an MO is localized on a given atom if the corresponding Fukui index is equal or greater than 0.1. We understand that some approximations of the Mulliken Population Analysis can generate problems but up today this approximation has worked satisfactorily. This is the physical basis of our concept of local molecular orbitals. Moreover, the way we build the data matrix for LRMA includes the fact that in large molecules electron donation may take place from different molecular orbitals. As an example, we present in Figs. 13 and 14 the HOMO-1 and HOMO of molecules 4 and 8.

ISSN: 0975-8585

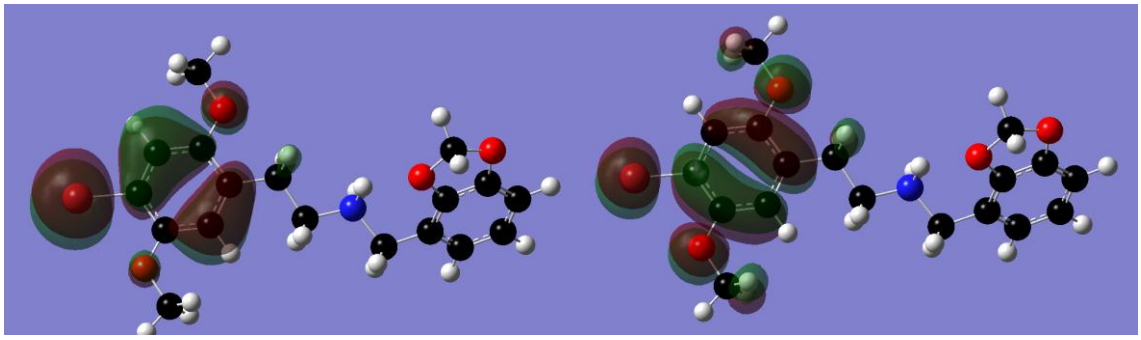

Figure 13. HOMO-1 (left) and HOMO (right) of molecule 4.

We can see that the HOMO and HOMO-1 are localized on ring A, allowing it to act as an electron-donor center. If ring B is engaged in a similar interaction, then the electrons located below the HOMO-1 should be involved. Observing the carbon atoms of ring A we can see that HOMO-1 and HOMO are fully not located on some of them. In these cases their local HOMO* or (HOMO-1)* do not coincide with the molecule's MOs.

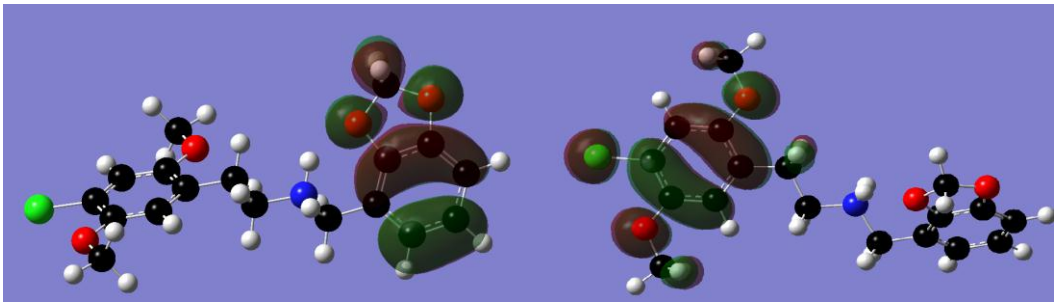

Figure 14. HOMO-1 (left) and HOMO (right) of molecule 8.

Here we can see that the HOMO is localized on ring A while HOMO-1 is localized on ring B. Therefore, both rings can act as electron-donor centers. Here there is a good example of local MOs: in ring B, and for some carbon atoms composing it, the local HOMO* corresponds to the molecule's (HOMO-1)*.

CONFORMATIONAL ASPECTS

We have seen in previous studies that, in general, the docked conformation does not coincide with the fully optimized geometries [73, 74, 94, 107]. To have a qualitative idea of the conformational flexibility of the molecules analyzed here, we show in Fig. 15 the superimposition of the ten lowest energy conformers of molecules 21 and 29. They were calculated with MarvinView software (Dreiding force field) and superimposed with Hyperchem [102, 108].

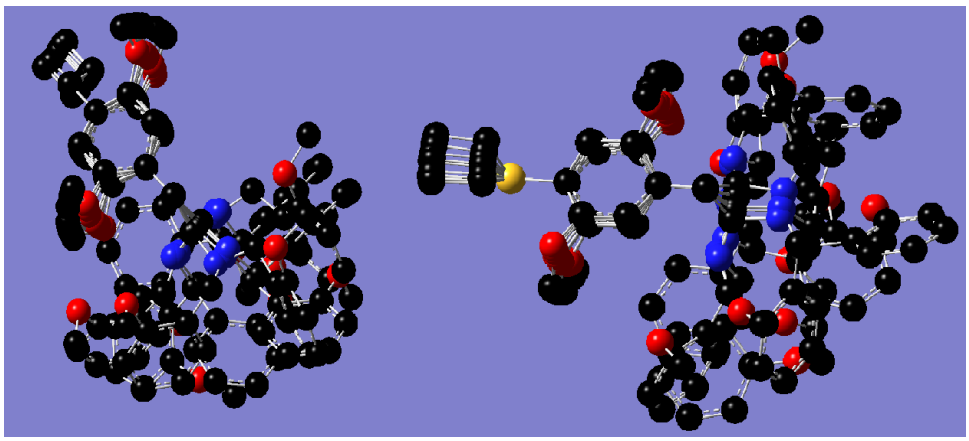

Figure 15. Superimposition of the ten lowest energy conformers of molecules 21 (left) and 29 (right).

We can see that, if we use ring A as the common structure for superimposition, the remaining part of the molecule has a relatively high degree of conformational freedom.

In summary, we have obtained satisfactory relationships between the electronic structure and 5-HT_{2C} receptor binding affinity for a group of N-Benzylphenethylamines. The partial interacting pharmacophore is built providing several ideas for the chemical modification of the molecules to obtain new structures with enhanced binding affinity.

REFERENCES

[1]. G Di Giovanni; E Esposito; V Di Matteo, 5-HT2C Receptors in the Pathophysiology of CNS Disease (The Receptors), Humana Press, New York, USA, 2012.
[2]. CA Marcinkiewcz; CE Dorrier; AJ Lopez; TL Kash, Neuropharmacol., 2015, 89, 157-167.
[3]. S Lopez-Esparza; LC Berumen; K Padilla; R Miledi; G García-Alcocer, Int. J. Dev. Neurosci., 2015, 42, 80-85.
[4]. CP Craige; S Lewandowski; LG Kirby; EM Unterwald, Neuropharmacol., 2015, 93, 41-51.
[5]. MA Vicente; H Zangrossi Jr, Neuropharmacol., 2014, 79, 127-135.
[6]. H Schellekens; AB Nongonierma; G Clarke; WEPA van Oeffelen; RJ FitzGerald, et al., Int. Dairy J., 2014, 38, 55-64.
[7]. CBP Martin; M Hamon; L Lanfumey; R Mongeau, Neurosci. Biobehav. Rev., 2014, 42, 208-223.
[8]. D Baptista-de-Souza; L Di Cesare Mannelli; M Zanardelli; L Micheli; RL Nunes-de-Souza, et al., Eur. J. Pharmacol., 2014, 735, 141-149.
[9]. V-M Papakosta; S Kalogerakou; D Kontis; E Anyfandi; E Theochari, et al., Behav. Brain Res., 2013, 243, 176-183.
[10]. S Ogino; Y Nagakura; M Tsukamoto; T Watabiki; T Ozawa, et al., Pharmacol. Biochem. Behav., 2013, 108, 8-15.
[11]. GA Higgins; EM Sellers; PJ Fletcher, Trends Pharmacol. Sci., 2013, 34, 560-570.
[12]. AA Scopinho; EAT Fortaleza; FMA Corrêa; LBM Resstel, Neuropharmacol., 2012, 63, 301-309.
[13]. RT O'Neil; RB Emeson, Neurobiol. Dis., 2012, 45, 8-13.
[14]. Q Li; T Luo; X Jiang; J Wang, Neuropharmacol., 2012, 62, 474-484.
[15]. PSdM Yamashita; VC de Bortoli; H Zangrossi Jr, Neuropharmacol., 2011, 60, 216-222.
[16]. E Sörman; D Wang; M Hajos; B Kocsis, Neuropharmacol., 2011, 61, 489-494.
[17]. K Nonogaki; M Suzuki; M Sanuki; M Wakameda; T Tamari, Biochem. Biophys. Res. Comm., 2011, 411, 445-448.
[18]. M Zaniewska; M Filip, Pharmacol. Rep., 2010, 62, Supplement 1, 10.
[19]. PJ Fletcher; J Sinyard; GA Higgins, Pharmacol. Biochem. Behav., 2010, 97, 170-178.
[20]. S Ahmad; K Ngu; KJ Miller; G Wu; C-p Hung, et al., Bioorg. Med. Chem. Lett., 2010, 20, 1128-1133.
[21]. K Yoshimoto; S Ueda; M Kobayasi; N Ishikawa; M Sakabe, et al., Neurosci. Res., 2009, 65, Supplement 1, S256.
[22]. NE Rowland; EM Crump; N Nguyen; K Robertson; Z Sun; RG Booth, Pharmacol. Biochem. Behav., 2008, 91, 176-180.
[23]. R Navarra; TA Comery; R Graf; S Rosenzweig-Lipson; M Day, Behav. Brain Res., 2008, 188, 412-415.
[24]. O Stiedl; I Misane; M Koch; T Pattij; M Meyer; SO Ögren, Neuropharmacol., 2007, 52, 949-957.
[25]. JA Siuciak; DS Chapin; SA McCarthy; V Guanowsky; J Brown, et al., Neuropharmacol., 2007, 52, 279-290.
[26]. C Wild; C Ding; G Zhang; N Anastasio; JS Moncrief, et al., Drug Alc. Depend., 2015, 146, e23.
[27]. RI Storer; PE Brennan; AD Brown; PJ Bungay; KM Conlon, et al., J. Med. Chem., 2014, 57, 5258-5269.
[28]. O Éliás; É Ágai-Csongor; G Domány; GM Keserű; A Gere, et al., Bioorg. Med. Chem. Lett., 2014, 24, 2118-2122.
[29]. G Zhao; C Kwon; SN Bisaha; PD Stein; KA Rossi, et al., Bioorg. Med. Chem. Lett., 2013, 23, 3914-3919.
[30]. HY Yang; J Tae; YW Seo; YJ Kim; HY Im, et al., European Journal of Medicinal Chemistry, 2013, 63, 558-569.
[31]. JM Fevig; J Feng; KA Rossi; KJ Miller; G Wu, et al., Bioorg. Med. Chem. Lett., 2013, 23, 330-335.
[32]. M Ettaoussi; A Sabaouni; M Rami; JA Boutin; P Delagrange, et al., European Journal of Medicinal Chemistry, 2012, 49, 310-323.
[33]. RJ Conway; C Valant; A Christopoulos; AD Robertson; B Capuano; IT Crosby, Bioorg. Med. Chem. Lett., 2012, 22, 2560-2564.

[34]. H Tye; SG Mueller; J Prestle; S Scheuerer; M Schindler, et al., Bioorg. Med. Chem. Lett., 2011, 21, 34-37.
[35]. N Renault; A Gohier; P Chavatte; A Farce, European Journal of Medicinal Chemistry, 2010, 45, 5086-5099.
[36]. N Krogsgaard-Larsen; AA Jensen; J Kehler, Bioorg. Med. Chem. Lett., 2010, 20, 5431-5433.
[37]. JY Kim; D Kim; SY Kang; W-K Park; HJ Kim, et al., Bioorg. Med. Chem. Lett., 2010, 20, 6439-6442.
[38]. DF Cummings; DC Canseco; P Sheth; JE Johnson; JA Schetz, Bioorg. Med. Chem., 2010, 18, 4783-4792.
[39]. PV Fish; AD Brown; E Evrard; LR Roberts, Bioorg. Med. Chem. Lett., 2009, 19, 1871-1875.
[40]. SJ Cho; NH Jensen; T Kurome; S Kadari; ML Manzano, et al., J. Med. Chem., 2009, 52, 1885-1902.
[41]. PE Brennan; GA Whitlock; DKH Ho; K Conlon; G McMurray, Bioorg. Med. Chem. Lett., 2009, 19, 4999-5003.
[42]. MD Andrews; MP Green; CMN Allerton; DV Batchelor; J Blagg, et al., Bioorg. Med. Chem. Lett., 2009, 19, 5346-5350.
[43]. CMN Allerton; MD Andrews; J Blagg; D Ellis; E Evrard, et al., Bioorg. Med. Chem. Lett., 2009, 19, 5791-5795.
[44]. I Shimada; K Maeno; Y Kondoh; H Kaku; K Sugasawa, et al., Bioorg. Med. Chem., 2008, 16, 3309-3320.
[45]. I Shimada; K Maeno; K-i Kazuta; H Kubota; T Kimizuka, et al., Bioorg. Med. Chem., 2008, 16, 1966-1982.
[46]. CM Park; SY Kim; WK Park; NS Park; CM Seong, Bioorg. Med. Chem. Lett., 2008, 18, 3844-3847.
[47]. HGF Richter; DR Adams; A Benardeau; MJ Bickerdike; JM Bentley, et al., Bioorg. Med. Chem. Lett., 2006, 16, 1207-1211.
[48]. S Röver; DR Adams; A Bénardeau; JM Bentley; MJ Bickerdike, et al., Bioorg. Med. Chem. Lett., 2005, 15, 3604-3608.
[49]. CJ Goodacre; SM Bromidge; D Clapham; FD King; PJ Lovell, et al., Bioorg. Med. Chem. Lett., 2005, 15, 4989-4993.
[50]. JS Gómez Jeria, Boll. Chim. Farmac., 1982, 121, 619-625.
[51]. JS Gómez-Jeria, Int. J. Quant. Chem., 1983, 23, 1969-1972.
[52]. JS Gómez-Jeria, "Modeling the Drug-Receptor Interaction in Quantum Pharmacology," in Molecules in Physics, Chemistry, and Biology, J. Maruani Ed., vol. 4, pp. 215-231, Springer Netherlands, 1989.
[53]. JS Gómez-Jeria; M Ojeda-Vergara; C Donoso-Espinoza, Mol. Engn., 1995, 5, 391-401.
[54]. JS Gómez-Jeria; M Ojeda-Vergara, J. Chil. Chem. Soc., 2003, 48, 119-124.
[55]. JS Gómez-Jeria, Elements of Molecular Electronic Pharmacology (in Spanish), Ediciones Sokar, Santiago de Chile, 2013.
[56]. JS Gómez-Jeria, Canad. Chem. Trans., 2013, 1, 25-55.
[57]. JS Gómez-Jeria; D Morales-Lagos, "The mode of binding of phenylalkylamines to the Serotonergic Receptor," in QSAR in design of Bioactive Drugs, M. Kuchar Ed., pp. 145-173, Prous, J.R., Barcelona, Spain, 1984.
[58]. JS Gómez-Jeria; DR Morales-Lagos, J. Pharm. Sci., 1984, 73, 1725-1728.
[59]. JS Gómez-Jeria; D Morales-Lagos; JI Rodriguez-Gatica; JC Saavedra-Aguilar, Int. J. Quant. Chem., 1985, 28, 421-428.
[60]. JS Gómez-Jeria; D Morales-Lagos; BK Cassels; JC Saavedra-Aguilar, Quant. Struct.-Relat., 1986, 5, 153-157.
[61]. JS Gómez-Jeria; P Sotomayor, J. Mol. Struct. (Theochem), 1988, 166, 493-498.
[62]. JS Gómez-Jeria; M Ojeda-Vergara, Int. J. Quant. Chem., 1997, 61, 997-1002.
[63]. JS Gómez-Jeria; L Lagos-Arancibia, Int. J. Quant. Chem., 1999, 71, 505-511.
[64]. JS Gómez-Jeria; L Lagos-Arancibia; E Sobarzo-Sánchez, Bol. Soc. Chil. Quím., 2003, 48, 61-66.
[65]. JS Gómez-Jeria; LA Gerli-Candia; SM Hurtado, J. Chil. Chem. Soc., 2004, 49, 307-312.
[66]. JS Gómez-Jeria; F Soto-Morales; J Rivas; A Sotomayor, J. Chil. Chem. Soc., 2008, 53, 1393-1399.
[67]. JS Gómez-Jeria, J. Chil. Chem. Soc., 2010, 55, 381-384.
[68]. T Bruna-Larenas; JS Gómez-Jeria, Int. J. Med. Chem., 2012, 2012 Article ID 682495, 1-16.
[69]. JS Gómez-Jeria, Der Pharm. Lett., 2014, 6., 95-104.
[70]. JS Gómez-Jeria; J Molina-Hidalgo, J. Comput. Methods Drug Des., 2014, 4, 1-9.
[71]. F Salgado-Valdés; JS Gómez-Jeria, J. Quant. Chem., 2014, 2014 Article ID 431432, 1-15.
[72]. R Solís-Gutiérrez; JS Gómez-Jeria, Res. J. Pharmac. Biol. Chem. Sci., 2014, 5, 1401-1416.
[73]. JS Gómez-Jeria; A Robles-Navarro, Der Pharma Chem., 2015, 7, 243-269.
[74]. JS Gómez-Jeria; A Robles-Navarro, Res. J. Pharmac. Biol. Chem. Sci., 2015, 6, 1811-1841.
[75]. C Barahona-Urbina; S Nuñez-Gonzalez; JS Gómez-Jeria, J. Chil. Chem. Soc., 2012, 57, 1497-1503.

[76]. DA Alarcón; F Gatica-Díaz; JS Gómez-Jeria, J. Chil. Chem. Soc., 2013, 58, 1651-1659.
[77]. JS Gómez-Jeria; M Flores-Catalán, Canad. Chem. Trans., 2013, 1, 215-237.
[78]. A Paz de la Vega; DA Alarcón; JS Gómez-Jeria, J. Chil. Chem. Soc., 2013, 58, 1842-1851.
[79]. I Reyes-Díaz; JS Gómez-Jeria, J. Comput. Methods Drug Des., 2013, 3, 11-21.
[80]. F Gatica-Díaz; JS Gómez-Jeria, J. Comput. Methods Drug Des., 2014, 4, 79-120.
[81]. JS Gómez-Jeria, Int. Res. J. Pure App. Chem., 2014, 4, 270-291.
[82]. JS Gómez-Jeria, Brit. Microbiol. Res. J., 2014, 4, 968-987.
[83]. JS Gómez-Jeria, SOP Trans. Phys. Chem., 2014, 1, 10-28.
[84]. JS Gómez-Jeria, Der Pharma Chem., 2014, 6, 64-77.
[85]. JS Gómez-Jeria, Res. J. Pharmac. Biol. Chem. Sci., 2014, 5, 2124-2142.
[86]. JS Gómez-Jeria, J. Comput. Methods Drug Des., 2014, 4, 32-44.
[87]. JS Gómez-Jeria, Res. J. Pharmac. Biol. Chem. Sci., 2014, 5, 424-436.
[88]. JS Gómez-Jeria, J. Comput. Methods Drug Des., 2014, 4, 38-47.
[89]. JS Gómez-Jeria, Res. J. Pharmac. Biol. Chem. Sci., 2014, 5, 780-792.
[90]. JS Gómez-Jeria; J Valdebenito-Gamboa, Der Pharma Chem., 2014, 6, 383-406.
[91]. D Muñoz-Gacitúa; JS Gómez-Jeria, J. Comput. Methods Drug Des., 2014, 4, 33-47.
[92]. D Muñoz-Gacitúa; JS Gómez-Jeria, J. Comput. Methods Drug Des., 2014, 4, 48-63.
[93]. DI Pino-Ramírez; JS Gómez-Jeria, Amer. Chem. Sci. J., 2014, 4, 554-575.
[94]. JS Gómez-Jeria; A Robles-Navarro, Res. J. Pharmac. Biol. Chem. Sci., 2015, 6, 1337-1351.
[95]. JS Gómez-Jeria; A Robles-Navarro, Res. J. Pharmac. Biol. Chem. Sci., 2015, 6, 755-783.
[96]. MS Leal; A Robles-Navarro; JS Gómez-Jeria, Der Pharm. Lett., 2015, 7, 54-66.
[97]. JS Gómez-Jeria, Res. J. Pharmac. Biol. Chem. Sci., 2015, 6, In press.
[98]. M Hansen, "Design and Synthesis of Selective Serotonin Receptor Agonists for Positron Emission Tomography Imaging of the Brain," Faculty of Pharmaceutical Sciences, vol. PhD Thesis, pp. 227, University of Copenhagen, Copenhagen, 2010.
[99]. MJ Frisch; GW Trucks; HB Schlegel; GE Scuseria; MA Robb, et al., G03 Rev. E.01, Gaussian, Pittsburgh, PA, USA, 2007.
[100]. JS Gómez-Jeria, D-Cent-QSAR: A program to generate Local Atomic Reactivity Indices from Gaussian 03 log files. 1.0, Santiago, Chile, 2014.
[101]. JS Gómez-Jeria, J. Chil. Chem. Soc., 2009, 54, 482-485.
[102]. Chemaxon, MarvinView, www.chemaxon.com, USA, 2014.
[103]. U Varetto, Molekel 5.4.0.8, Swiss National Supercomputing Centre: Lugano, Switzerland, 2008.
[104]. RD Dennington; TA Keith; JM Millam, GaussViev 5.0.8, GaussViev 5.0.8, 340 Quinnipiac St., Bldg. 40, Wallingford, CT 06492, USA, 2000-2008.
[105]. Statsoft, Statistica 8.0, 2300 East 14 th St. Tulsa, OK 74104, USA, 1984-2007.
[106]. JS Gómez-Jeria, Acta sud Amer. Quím., 1984, 4, 1-9.
[107]. JS Gómez-Jeria; A Robles-Navarro, Der Pharma Chem., 2015, 7, 230-241.
[108]. Hypercube, Hyperchem 7.01, 419 Phillip St., Waterloo, Ontario, Canada, 2002.